

Robust Visual Robot Localization Across Seasons using Network Flows

Tayyab Naseer

University of Freiburg
naseer@cs.uni-freiburg.de

Luciano Spinello

University of Freiburg
spinello@cs.uni-freiburg.de

Wolfram Burgard

University of Freiburg
burgard@cs.uni-freiburg.de

Cyrill Stachniss

University of Bonn
cyrill.stachniss@igg.uni-bonn.de

Abstract

Image-based localization is an important problem in robotics and an integral part of visual mapping and navigation systems. An approach to robustly match images to previously recorded ones must be able to cope with seasonal changes especially when it is supposed to work reliably over long periods of time. In this paper, we present a novel approach to visual localization of mobile robots in outdoor environments, which is able to deal with substantial seasonal changes. We formulate image matching as a minimum cost flow problem in a data association graph to effectively exploit sequence information. This allows us to deal with non-matching image sequences that result from temporal occlusions or from visiting new places. We present extensive experimental evaluations under substantial seasonal changes. Our approach achieves accurate matching across seasons and outperforms existing state-of-the-art methods such as FABMAP2 and SeqSLAM.

Introduction

Recognizing a previously seen place is an important and challenging problem in robotics and computer vision. The ability to reliably relocalize is a prerequisite for most simultaneous localization and mapping (SLAM) systems and for visual navigation. A series of robust approaches have been proposed in the past including FAB-MAP2 (Cummins and Newman 2009), SeqSLAM (Milford and Wyeth 2012), SP-ACP (Neubert, Sunderhauf, and Protzel 2013), and FrameSLAM (Agrawal and Konolige 2008). Some of these methods have been shown to robustly recognize previously seen locations even under a wide spectrum of visual changes including dynamic objects, different illumination, and varying weather conditions.

In this paper, we address the problem of visual localization across seasons using image sequences collected along routes. This is, for example, important for localizing a vehicle in winter even though the reference images have been recorded in summer. In this sense, our approach aims at similar goals as SeqSLAM (Milford and Wyeth 2012) and SP-ACP (Neubert, Sunderhauf, and Protzel 2013), i.e., visual



Figure 1: Two images of the same place in different seasons that are successfully matched by our approach.

route recognition over different seasons by exploiting the sequential nature of the data.

The main contribution of this paper is a novel approach that operates *without* using any GPS or odometry information, that does not require any season-based feature learning, that supports vehicles which travel at different speeds, that can handle revisits of places and loop closures, and that can handle partial route matching. Furthermore, it can operate with imagery taken at low frame rates (~ 1 Hz), does not assume a pixel accurate alignment of the images, does not require perfect initialization of the route, and has no initial learning phase, e.g., for building a dictionary. The advantage of our method is that it simultaneously achieves all of these objectives, which makes it applicable in a more general context. Fig. 1 shows a successful match of the same place across seasons.

To achieve a robust localization, we use an image description that builds upon a dense grid of HOG descriptors (Dalal and Triggs 2005). We build a data association graph that relates images from sequences retrieved in different seasons. In this way, we compute multiple route hypotheses, deal with occlusions over short periods of time, and handle deviations from the previously taken route. We solve the visual place recognition problem by computing network flows in the association graph and generate multiple vehicle route hypotheses. By exploiting the specific structure of our graph, we solve this problem efficiently. Our experimental evaluation suggests, that our method is an effective tool to perform visual localization across seasons. Under these conditions, it outperforms the current state-of-the-art methods SeqSLAM and FABMAP2.



Figure 2: Feature-based matching of the same place across seasons. In this example, SURF features do not match reliably due to a substantial visual change.

Related Work

Visual localization has a long history in computer vision and robotics, see Fuentes-Pacheco, Ruiz-Ascencio, and Rendón-Mancha (2012) for a recent survey. Large environmental and seasonal variations are a major bottleneck towards robust and long-term visual navigation. Various approaches have been proposed to localize autonomous robots using visual input (Cummins and Newman 2009; Davison et al. 2007; Agrawal and Konolige 2008; Bennewitz et al. 2006). Visual localization with extreme perceptual variations has been recognized as a major obstacle for persistent autonomous navigation and has been addressed by different researchers (Glover et al. 2010; Cummins and Newman 2009). Biber and Duckett (2005) deal with changing indoor environments by sampling laser maps at multiple time scales. Each sample of the map at a particular timescale is maintained and updated using the sensor data of the robot. This allows them to model spatio-temporal variations in the map. Stachniss and Burgard (2005), in contrast, aim at modeling different instances of typical states of the world using a clustering approach. Many of the visual place recognition approaches rely on image matching by using features such as SURF (Bay et al. 2008) and SIFT (Lowe 2004). Such feature-based algorithms work reliably for matching images that undergo rotation and scale variations but perform poor under extreme perceptual changes. Valgren and Lilienthal (2010) made an attempt to use both features in combination with geometric keypoint constraints for across-seasons image matching. For our datasets, we found that SIFT and SURF features do not match robustly, see Fig. 2 for an example. As a result, methods such as FAB-MAP2 by Cummins and Newman (2009) that require a reliable matching of these features tend to fail. Furgale and Barfoot (2010) propose a teach and repeat system for long term autonomy using stereo vision. They create series of submaps during the teach phase which relaxes the need of accurate global reconstruction while repeating the routes. Although, this approach allows for navigating over longer routes, it does not address large perceptual changes from the original traverse.

The goal of the work of Milford and Wyeth (2012), which has a similar overall aim as our approach, is to match a sequence of query images to a sequence of database images. The method computes a matching matrix which stores dissimilarity scores between all images in a query and database sequence. The straight-line path through this matrix with the minimum sum of dissimilarity scores across image pairs results in the best matched route. This corresponds to the as-

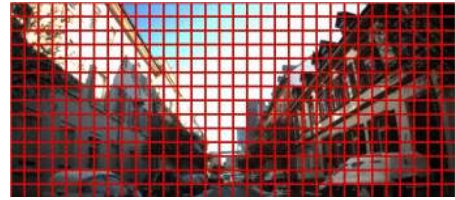


Figure 3: Tessellation into cells for computing the image descriptor. A HOG feature is computed in each cell.

sumption of a linear velocity of the vehicle within each sequence. This assumption, however, is often violated in real urban environments and robot applications. Neubert, Sunderhauf, and Protzel (2013) propose to combine an appearance change prediction with a vocabulary-based method to predict how the visual word in the current scene would appear under changes. For learning the appearance changes across seasons, an accurate image alignment is needed. Johns and Yang (2013) learn discriminative statistics on the co-occurrence of features over different conditions. This requires to learn stable and discriminative features over different times of the day or over different seasons. In our experiments, however, we were unable to obtain such stable and discriminative features under the strong seasonal changes that we experienced. Instead of explicitly addressing the visual place recognition with extreme perceptual differences, Churchill and Newman (2012) associate different appearances, which they call as experiences, to the same place. They localize in previously learnt experiences and associate a new experience in case of a localization failure. At least during the setup phase, this requires some degree of place knowledge to assign a new experience to an existing place.

Our approach uses network flows to consider the sequential nature of the data in the individual routes. In other fields, network flows have been successfully used to address data association problems when tracking multiple people (Zhang, Li, and Nevatia 2008; Ben Shitrit et al. 2013).

Visual Route Matching Across Seasons

We define the set $\mathcal{D} = (d_1, \dots, d_D)$ as the temporally ordered set of images that constitutes the visual map of places (the database) and $D = |\mathcal{D}|$. The set $\mathcal{Q} = (q_1, \dots, q_Q)$ with $Q = |\mathcal{Q}|$ refers to the query sequence that was recorded in a different season or after a substantial scene change.

Matching Images

Matching images of the same place between seasons is a non-trivial task. The appearance of the same place is likely to change substantially over the time of the year, see Fig. 1 for an example. Variations occur due to different weather conditions, changing illumination, or other kinds of scene change such as construction sites, new buildings, etc. In most real world applications, re-visiting the same place typically happens under different conditions: the view-point of the camera is not the same, the vehicle moves at different speeds, and the framerate of the camera may differ. In particular, different seasonal weather conditions tend to have

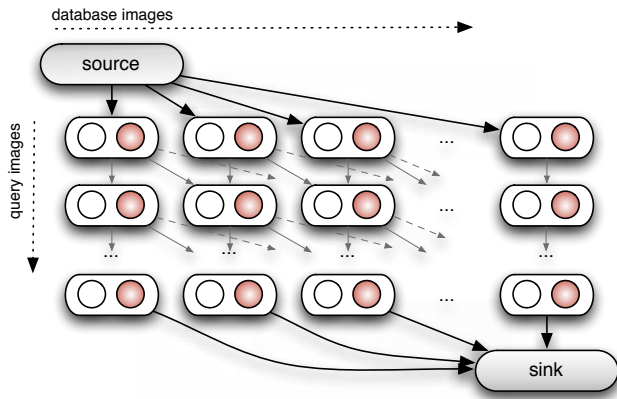


Figure 4: Illustration of the data association graph.

large impact on image-retrieval-based place recognition. For example, during a snowy winter day, the landscape is covered by snow and the scene is poorly illuminated, yielding few texture and low contrast. These settings cause images to have weak gradients, which is suboptimal for computing distinctive image descriptors. For this reason, place recognition methods that make use of keypoint-based feature detectors to compute region descriptors (Mikolajczyk et al. 2005) are likely to detect only a small number of keypoints. The scarcity of keypoints in turn yields only a limited number of feature comparisons between images resulting in poor matchings. Instead of relying on keypoints, we compute for each image a fixed quantity of descriptors. To achieve this, we tessellate the image into a grid of regular cells, see Fig. 3. For each cell, we compute a HOG descriptor and combine all descriptors into a single, dense description of the whole image. The overall image descriptor \mathbf{h} is a vector composed of the concatenation of all the histograms of gradients computed on all the cells.

The resulting image descriptor is view-point dependent due to the choice of the tessellation. To deal with this problem, we use large grid cells of 32×32 pixels in a 640×480 image. This decision is motivated by the particular choice of HOG as grid feature. HOG describes a region by accumulating the gradient regardless to its location. As soon as the same subject appears in the same cell, it is likely that its descriptor is similar when the subject is seen from two similar viewpoints. Moreover, the usage of HOG enables matching under a range of different viewpoints and image conditions (Dalal and Triggs 2005).

The distance between image $q_i \in \mathcal{Q}$ and $d_j \in \mathcal{D}$ is computed by the cosine distance of the two image descriptors, respectively \mathbf{h}_{q_i} and \mathbf{h}_{d_j} :

$$c_{ij} = \frac{\mathbf{h}_{d_j} \cdot \mathbf{h}_{q_i}}{\|\mathbf{h}_{d_j}\| \|\mathbf{h}_{q_i}\|}, \quad (1)$$

where $c_{ij} \in [0, 1]$ and $c_{ij} = 1$ indicates a perfect match. The matching matrix \mathbf{C} has a size of $Q \times D$ and consists of all c_{ij} , i.e., the cosine distances between all images of \mathcal{Q} and \mathcal{D} , computed according to Eq. (1).

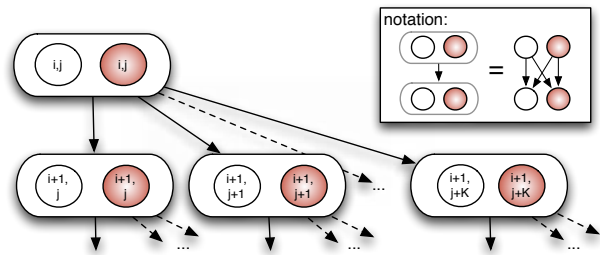


Figure 5: Illustration of the connections \mathcal{E}^a and \mathcal{E}^b between matching (white) and hidden (red) nodes. The white rounded rectangles are only used for illustration: an edge between two rounded rectangles means that all nodes contained in the first rectangle are connected via a directed edge to all nodes in the second rectangle.

Building the Data Association Flow Network

A standard approach to image-based localization returns for a query image in \mathcal{Q} the best matching image in \mathcal{D} according to the matching matrix \mathbf{C} . Due to the visual change across seasons, a best-match-strategy in \mathbf{C} typically results in a poor localization performance. In this paper, we leverage that \mathcal{Q} and \mathcal{D} consist of *image sequences* that are recorded on a robot or vehicle. As a result, locations are visited progressively and images are not in random order. The matching patterns in the matching matrix \mathbf{C} reflect the temporal information of both sequences. Our approach exploits the sequential nature of data but does not assume that every image in \mathcal{Q} has a matching counterpart in \mathcal{D} . We consider sequences that can start and stop at any position in the query and database set. Both sets might be composed of images that have been recorded at different framerates or while traveling at different speeds.

In this paper, we propose to solve the visual route localization problem by building a flow network and computing its minimum cost flow. The minimum cost flow problem consists of determining the most cost-effective way for sending a fixed amount of flow through a network (Ahuja, Magnanti, and Orlin 1993). The flow network is a directed graph with at least one source node and one sink node. The source node is the one that produces flow and the sink node is the one that consumes flow. To each edge, we associate a cost w and a capacity r . A source node is connected by only outgoing edges, a sink node by only ingoing edges. The capacity defines the number of units that can flow over an edge. Our idea is to build a flow network to model the possible matches between \mathcal{D} and \mathcal{Q} . A minimum cost flow algorithm finds a set of paths that connect the source to the sink minimizing the path cost while transporting the specified flow to the sink. Those paths represent multiple hypothesis about the correct image matching and the estimation of the vehicle route. In order to match complex temporal sequences that include loops, we introduce special nodes to allow solutions that include partially matched sequences.

In our approach, the network is a graph $\mathcal{G} = (\mathcal{X}, \mathcal{E})$, where \mathcal{X} are the nodes and \mathcal{E} the edges. We denote the quantity of flow generated by the source node as $F \in \mathbb{N}$.

Nodes The set \mathcal{X} contains four types of nodes: the *source* x^s , the *sink* x^t , the *matching nodes* x_{ij} , and so-called *hidden nodes* \check{x}_{ij} . The node x^s is the node that creates all the flow F and x^t is the only sink that consumes it. A node x_{ij} represents a match between the i -th image in \mathcal{Q} and the j -th image \mathcal{D} , i.e., that both images are from the same location. There exists a hidden node \check{x}_{ij} for each matching node x_{ij} . The hidden nodes represent “non-matches” between images and such nodes allow for paths even though the image pairs cannot be matched. These nodes are traversed during short temporal occlusions or non-matching sequences that occur when the robot deviates from the original route.

Edges The edges in \mathcal{G} define the possible ways of traversing the graph from the source to the sink. Fig. 4 illustrates the connectivity of our graph. We define four types of edges in $\mathcal{E} = \{\mathcal{E}^s, \mathcal{E}^t, \mathcal{E}^a, \mathcal{E}^b\}$. The first set \mathcal{E}^s connects the source to a matching node or to hidden node:

$$\mathcal{E}^s = \{(x^s, x_{1j}), (x^s, \check{x}_{1j})\}_{j=1, \dots, D} \quad (2)$$

The set \mathcal{E}^s models that the first image of \mathcal{Q} can be matched with any image in the \mathcal{D} via the matching nodes or that no match is found via the hidden nodes. The second set of edges, \mathcal{E}^t , represents all the connections that go to the sink:

$$\mathcal{E}^t = \{(x_{Qj}, x^t), (\check{x}_{Qj}, x^t)\}_{j=1, \dots, D} \quad (3)$$

The sink can be reached from any of the matching nodes x_{Qj} and from the corresponding hidden nodes \check{x}_{Qj} with $j = 1, \dots, D$. This models the matching or non-matching of the last query image.

The set \mathcal{E}^a of edges establishes the connections between the matching nodes as well as between the hidden nodes

$$\mathcal{E}^a = \{(x_{ij}, x_{(i+1)k}), (\check{x}_{ij}, \check{x}_{(i+1)k})\}_{\substack{i=1, \dots, Q, j=1, \dots, D, \\ k=j, \dots, (j+K), k \leq D}} \quad (4)$$

where $k = j, \dots, (j + K)$. These edges allow for finding sequences of matching images or sequences of unmatched query images respectively. Finally, the last set \mathcal{E}^b of edges connects hidden and matching nodes

$$\mathcal{E}^b = \{(x_{ij}, \check{x}_{(i+1)k}), (\check{x}_{ij}, x_{(i+1)k})\}_{\substack{i=1, \dots, Q, j=1, \dots, D, \\ k=j, \dots, (j+K), k \leq D}} \quad (5)$$

The edges in \mathcal{E}^b are the ones that are traversed when the sequence is not continued with the children of a node. Edges in \mathcal{E}^b are the ones that are traversed when a matching is found again so that the matching sequence can continue. See Fig. 5 for an illustration of the edges in \mathcal{E}^a and \mathcal{E}^b . As a design decision, there are no edges connecting nodes back in time, mainly for constraining the search space. However, this is not a limiting factor: loops in the route can be found by solving the flow network when $F > 1$.

The value of K specifies the number of considered path hypotheses exiting from each node: the fan-out from a vertex defines which of the subsequent images can be concatenated to a path. Values for $K > 1$ allow for matching sequences recorded at different vehicle speeds or in case of different camera framerates. An edge between nodes (i, j) and $(i+1, j)$ models a vehicle that does not move. In our implementation, we use $K = 4$, which seems to be a sufficient

value for typical city-like navigation scenarios. Edges connected to hidden states capture the fact that the corresponding images cannot be matched (due to strong changes, occlusions, etc.), but allow the path to continue through some hidden nodes. The hidden nodes can also be used to terminate a matching sequence without terminating the overall localization process. This is important to handle situations in which the vehicle temporarily deviates from the route taken during mapping. Thanks to this graph design, \mathcal{G} is a directed acyclic graph (DAG).

Edge Costs and Capacity The cost of an edge connected to a matching node x_{ij} is $w_{ij} = \frac{1}{c_{ij}}$, where c_{ij} is computed in Eq. (1). In case that the edge is connected to an hidden node, the weight is constant, $\check{w} = W$. We determined this parameter experimentally by using a precision-recall evaluation. In addition to that, we set the weight of the edges in \mathcal{E}^s and \mathcal{E}^t to 0.

All edges that interconnect the hidden nodes have a capacity $r = F + 1$ so that they can be considered for usage for each unit of flow. All the other edges have a capacity of $r = 1$ so that they can be only used once. The path resulting from the minimum cost flow on \mathcal{G} corresponds to the best data association between \mathcal{D} and \mathcal{Q} .

Minimum Cost Flow For Vehicle Localization

In this section, we provide a probabilistic interpretation of our solution for solving this problem. Without loss of generality, we present a formulation for $F = 1$. We define the ordered set $\mathcal{A} = (x^s, x_{a_1}, \dots, x_{a_A}, x^t)$ where x_{a_i} is a simplified notation indicating a vertex in \mathcal{X} . The sequence \mathcal{A} is a route hypothesis, i.e., a sequence of matched images between seasons. It contains only vertices that can be connected with the edges presented in the previous section. Each sequence starts at the source and ends at the sink. For finding the best matching visual route, we find the optimal sequence \mathcal{A}^* with a maximum a posteriori approach:

$$\begin{aligned} \mathcal{A}^* &= \operatorname{argmax}_{\mathcal{A}} p(\mathcal{A} | \mathcal{X}) \\ &= \operatorname{argmax}_{\mathcal{A}} p(\mathcal{X} | \mathcal{A}) p(\mathcal{A}) \\ &= \operatorname{argmax}_{\mathcal{A}} \prod_i p(x_i | \mathcal{A}) p(\mathcal{A}) \end{aligned} \quad (6)$$

We consider all the likelihood probabilities to be conditionally independent given \mathcal{A} and define the prior $p(\mathcal{A})$ as

$$p(\mathcal{A}) = p_s p(x_{a_2} | x_{a_1}) \dots p(x_{a_A} | x_{a_{A-1}}) p_t \quad (7)$$

where p_s and p_t are the priors associated to the source and sink. The term $p(x_{a_{i+1}} | x_{a_i})$ is proportional to $c_{a_{i+1}}$. We define the likelihood $p(x_i | \mathcal{A})$ of x_i being part of \mathcal{A} as

$$p(x_i | \mathcal{A}) = \begin{cases} 1/Q & \text{if } x_i \in \mathcal{A} \\ 0 & \text{otherwise.} \end{cases} \quad (8)$$

To search for the best solution of Eq. (6), we use a minimum cost flow solver. An efficient implementation for minimum cost flow is the one of Goldberg and Kennedy (1995), which has complexity $\mathcal{O}(|\mathcal{X}|^2 |\mathcal{E}| \log |\mathcal{X}|)$. In our context,

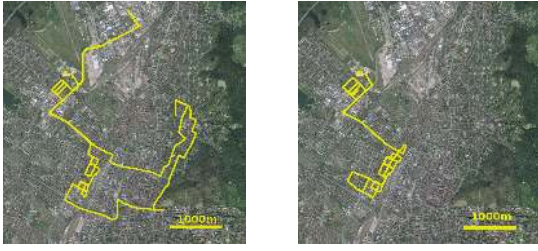


Figure 6: Two datasets visualized in a satellite image. The vehicle route is shown in yellow.

this is expensive as typical problems consist of hundreds or thousands of images. Note that in the special case of $F = 1$, finding a minimal cost flow is equivalent to find the shortest path.

To solve this problem efficiently, we exploit the specific structure of the graph. Our graph \mathcal{G} is a DAG with non-negative edges and each edge has either a capacity $r = 1$ or $r = F + 1$. This means that all paths through the matching nodes found by the minimum cost network flow consist in *different* paths. Given these restrictions, we formulate an equivalent solution with a substantially smaller computational complexity. Computing a shortest path in a DAG with a single source can be done by topological sorting in $\mathcal{O}(|\mathcal{X}| + |\mathcal{E}|)$, which is even more efficient than Dijkstra’s or the Bellman-Ford algorithm. Note that, in our case, $|\mathcal{E}|$ depends linearly with respect to $|\mathcal{X}|$. For depleting all flow of the source node, we repeat this procedure F times. This leads to an overall complexity of $\mathcal{O}(F|\mathcal{X}|) = \mathcal{O}(FQD)$.

Each execution of the solver leads to a loop-free path of the vehicle, as a consequence of our graph connectivity. The flow F controls the maximum number of vehicle path hypotheses that are found in the graph. As there are at most F iterations, the system returns the F best paths. In this way, we are able to report sequences that include up to F traversals of the same loop. The parameter F is either set beforehand by limiting the search to F possible solutions or by repeating the search until the computed path is dominated by hidden nodes (non-matching events).

Experimental Evaluation

Our evaluation shows that our approach accurately matches image sequences across seasons and it outperforms two state-of-the-art methods such as FABMAP2 and SeqSLAM. For the evaluation, we recorded datasets by driving through a city with a camera-equipped car during summer and winter. The datasets contain overlapping routes, typical acceleration and breaking maneuvers, other traffic participants, variations in the camera pose, and seasonal as well as structural changes in the environment. Fig. 6 illustrates the circa 50 km long traveled path on a satellite map. The datasets contain between 6,915 and 30,790 images. During summer, we mounted the camera outside the car, whereas during winter we installed it behind the windshield. For evaluation, we manually annotated a set of corresponding winter-summer image pairs. No rectification, cropping, or other preprocess-

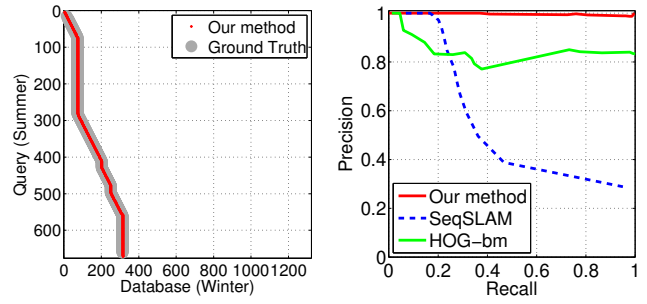


Figure 7: Left: Ground truth (thick) and our matching results (dots). Right: Precision recall curve. Our approach accurately estimates the vehicle route and outperforms OpenSeqSLAM and the HOG-based best match strategy.

ing has been applied to the images.

Experimental Results

The first experiment is designed to illustrate that our method is well-suited to perform matching across seasons. For this experiment, we used a sequence of 676 summer and 1,322 winter images including labels corresponding to a track length of around 3 km. The car drove approximately along the same route but with different speeds and due to traffic, it had to stop a few times at different locations while acquiring the query images. The sequence does not include any loop and each query image has a matching counterpart in the database. Fig. 1 shows a pair of images from this sequence.

The manually labeled ground truth matches in both sequences as well as our result are shown in the left image of Fig. 7. For the evaluation, we accept a match if the resulting true match is off by up to two images. We quantify the performance of our approach by using a precision-recall curve, see the right image of Fig. 7. We compare against SeqSLAM, which is the current state of the art in cross-season image matching, by using the OpenSeqSLAM implementation (Sunderhauf, Neubert, and Protzel 2013). The curve “HOG-bm” refers to selecting the best match above a threshold using our tessellation-based HOG descriptor matching in Eq. (1) without using the data association graph.

Our approach matches the summer and winter sequences at a high degree of accuracy with precision and recall values close to 1. It also successfully estimates the route of the vehicle even though the car was moving at different speeds and stopped several times during the query run. Our approach is up to 3 times better in precision than OpenSeqSLAM and it reaches ~ 0.95 Equal Error Rate (EER). The Equal Error Rate is a measure of performance on precision-recall graphs. OpenSeqSLAM achieves comparable precision results only at low recall rates. At increasing recall rates, OpenSeqSLAM decreases in precision.

A second image sequence consists of 1,322 winter images (\mathcal{D}) and 441 summer images (\mathcal{Q}). This dataset is more challenging as the matching sequence is interrupted and the vehicle visited places in \mathcal{Q} that have not been visited in \mathcal{D} and vice versa. Ground truth and our results as well as the precision-recall curves are shown in Fig. 8.

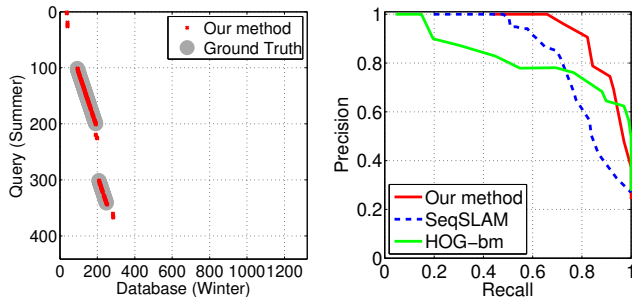


Figure 8: Sequence in which the robot visits new places. Left: Ground truth (thick) and our matching results (dots). Right: Precision recall curve. Our approach outperforms SeqSLAM and the HOG-based best match strategy in such scenarios.

Our approach again clearly outperforms OpenSeqSLAM. It is up to 1.5 times better in precision than OpenSeqSLAM and it reaches ~ 0.82 EER. It also correctly estimates the route of the vehicle even though not all query images match the database. This means that the solution includes a path through the data association graph that traverses hidden nodes. From the hidden nodes, the path switched back to matching nodes and continued to correctly match other images in the database.

Additionally, we compare our method to FABMAP2, another successful state-of-the-art method for place recognition. For the comparison to FABMAP2, we used the OpenFABMAP2 implementation by Glover et al. (2012). The original binary version of FABMAP2 provided by the Oxford Mobile Robotics Group (Cummins and Newman 2009) performs similar to OpenFABMAP2. For the sake of brevity, results are reported only once. The results of OpenFABMAP2 are shown in Fig. 9. No meaningful matches are found by OpenFABMAP2. We believe that may be caused by the use of keypoint-based feature detectors in FABMAP2. As explained above, those may be suboptimal for matching across seasons, e.g., see Fig. 2.

For the last experiment, we selected a database of 596 images from winter and 1,213 images from summer. This

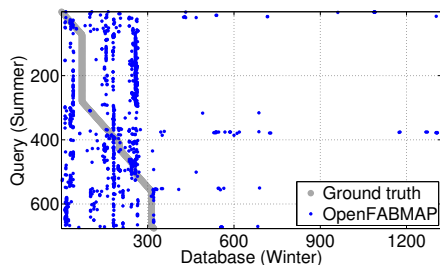


Figure 9: OpenFABMAP2 results obtained by matching the query images with the database without creating new places, i.e., localization-only mode. Only few correct matches are found by OpenFABMAP2. This is probably caused by using SURF features for matching places across seasons.

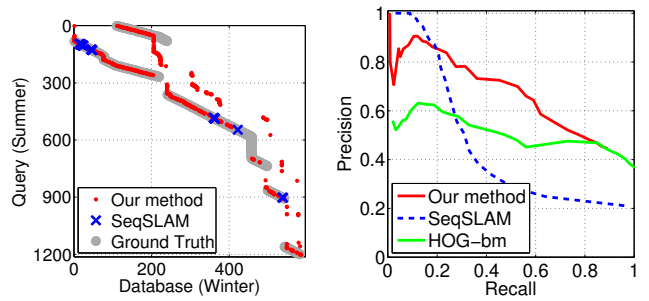


Figure 10: Left: Ground truth (thick), our matching results (dots), and OpenSeqSLAM (cross). Right: Precision recall curve for the third dataset. Even though the query set contain loops and places that are not in the database, our approach is accurate and it outperforms SeqSLAM and the HOG-based best match strategy.

dataset is the most challenging one as it contains loops as well as places that the car never visited while building \mathcal{D} . Our approach is up to 2 times better in precision than OpenSeqSLAM and it reaches ~ 0.6 EER by using a flow of $F = 2$ as shown in Fig. 10. This illustrates that our approach is able to estimate the vehicle route even in the case of place revisits and loops. At low recall-rates, our approach has lower accuracy but its advantage becomes clear as soon as the recall-rate increases. In contrast to that, OpenSeqSLAM is not able to handle loops. In conclusion, our approach outperforms the state-of-the-art methods FABMAP2 and SeqSLAM.

Finally, our approach shows a comparable runtime to SeqSLAM. In all the experiments our approach takes between 2.1s and 3.7s on a regular PC using a single core.

Conclusions

We addressed the problem of visual localization by using image sequences. We proposed a novel approach that is designed to perform localization even under substantial seasonal changes, e.g., summer vs. winter. We addressed the problem by a HOG-based description of the images combined with a directed acyclic data association graph. We formulated the problem of matching image sequences over seasons as a minimum cost network flow problem and also solved the issue of dealing with non-matching image sequences that may result from collecting data at new places. Our experimental results suggest that our approach allows for accurate and robust matching across seasons and that it outperforms existing state-of-the-art methods such as FABMAP2 and SeqSLAM in this setting.

Acknowledgements

This work has partly been supported by the European Commission under FP7-ICT-600890-ROVINA, FP7-ICT-610603-EUROPA2, and ERC-AG-PE7-267686-LIFENAV. In addition to that, the authors would like to thank Noha Radwan for her support during the experimental evaluation.

References

- Agrawal, M., and Konolige, K. 2008. Frameslam: From bundle adjustment to real-time visual mapping. *IEEE Transactions on Robotics* 24(5).
- Ahuja, R. K.; Magnanti, T. L.; and Orlin, J. B. 1993. *Network flows: theory, algorithms, and applications*. Prentice hall.
- Bay, H.; Ess, A.; Tuytelaars, T.; and Van Gool, L. 2008. Speeded-up robust features (SURF). *Comput. Vis. Image Underst.* 110(3):346–359.
- Ben Shitrit, H.; Berclaz, J.; Fleuret, F.; and Fua, P. 2013. Multi-commodity network flow for tracking multiple people. *IEEE Trans. Pattern Anal. Mach. Intell.* 99:1.
- Bennewitz, M.; Stachniss, C.; Burgard, W.; and Behnke, S. 2006. Metric localization with scale-invariant visual features using a single perspective camera. In *European Robotics Symposium*, 143–157.
- Biber, P., and Duckett, T. 2005. Dynamic maps for long-term operation of mobile service robots. In *Proc. of Robotics: Science and Systems*, 17–24. The MIT Press.
- Churchill, W., and Newman, P. 2012. Practice makes perfect? managing and leveraging visual experiences for life-long navigation. In *Proc. of the IEEE Int. Conf. on Robotics and Automation (ICRA)*.
- Cummins, M., and Newman, P. 2009. Highly scalable appearance-only SLAM - FAB-MAP 2.0. In *Proc. of Robotics: Science and Systems*.
- Dalal, N., and Triggs, B. 2005. Histograms of oriented gradients for human detection. In *Proc. of the IEEE Int. Conf. on Computer Vision and Pattern Recognition (CVPR)*.
- Davison, A. J.; Reid, I. D.; Molton, N. D.; and Stasse, O. 2007. Monoslam: Real-time single camera slam. *IEEE Trans. Pattern Anal. Mach. Intell.* 29:2007.
- Fuentes-Pacheco, J.; Ruiz-Ascencio, J.; and Rendón-Mancha, J. 2012. Visual simultaneous localization and mapping: a survey. *Artificial Intelligence Review* 1–27.
- Furgale, P. T., and Barfoot, T. D. 2010. Visual teach and repeat for long-range rover autonomy. *Int. J. Field Robotics* 27:534–560.
- Glover, A.; Maddern, W.; Milford, M.; and Wyeth, G. 2010. FAB-MAP + RatSLAM: Appearance-based slam for multiple times of day. In *Proc. of the IEEE Int. Conf. on Robotics and Automation (ICRA)*, 3507–3512.
- Glover, A. J.; Maddern, W. P.; Warren, M.; Reid, S.; Milford, M.; and Wyeth, G. 2012. Openfabmap: An open source toolbox for appearance-based loop closure detection. In *Proc. of the IEEE Int. Conf. on Robotics and Automation (ICRA)*.
- Goldberg, A. V., and Kennedy, R. 1995. An efficient cost scaling algorithm for the assignment problem. *Mathematical Programming* 71(2):153–177.
- Johns, E., and Yang, G.-Z. 2013. Feature co-occurrence maps: Appearance-based localisation throughout the day. In *Proc. of the IEEE Int. Conf. on Robotics and Automation (ICRA)*.
- Lowe, D. 2004. Distinctive image features from scale-invariant keypoints. *Int. J. Comput. Vision* 60(2):91–110.
- Mikolajczyk, K.; Tuytelaars, T.; Schmid, C.; Zisserman, A.; Matas, J.; Schaffalitzky, F.; Kadir, T.; and Gool, L. V. 2005. A comparison of affine region detectors. *Int. J. Comput. Vision* 65:2005.
- Milford, M., and Wyeth, G. F. 2012. Seqslam: Visual route-based navigation for sunny summer days and stormy winter nights. In *Proc. of the IEEE Int. Conf. on Robotics and Automation (ICRA)*.
- Neubert, P.; Sunderhauf, N.; and Protzel, P. 2013. Appearance change prediction for long-term navigation across seasons. In *Proc. of the European Conference on Mobile Robotics (ECMR)*.
- Stachniss, C., and Burgard, W. 2005. Mobile robot mapping and localization in non-static environments. In *Proc. of the National Conference on Artificial Intelligence (AAAI)*, 1324–1329.
- Sunderhauf, N.; Neubert, P.; and Protzel, P. 2013. Are we there yet? challenging seqslam on a 3000 km journey across all four seasons. In *Proc. of the ICRA Workshop on Long-Term Autonomy*.
- Valgren, C., and Lilienthal, A. 2010. SIFT, SURF & Seasons: Appearance-based long-term localization in outdoor environments. *Robotics and Autonomous Systems* 85(2):149–156.
- Zhang, L.; Li, Y.; and Nevatia, R. 2008. Global data association for multi-object tracking using network flows. In *Proc. of the IEEE Int. Conf. on Computer Vision and Pattern Recognition (CVPR)*.